Journal of the Serbian Chemical Society
JSCS-info@shd.org.rs • www.shd.org.rs/JSCS
J. Serb. Chem. Soc. *86* (9) 859–870 (2021)
JSCS–5467
Original scientific paper
Published 11 February, 2021

Benzimidazole-functionalized fluorescent probe for rapid detection of 2,4,6-trinitrophenol and Ag^+ in semiaqueous medium

BIN WANG[1–3], FAN JIANG[1], XIXI ZUO[1], JING MA[1] and XIANGMEI MA[1,2]*

[1]*Institute of Chemical Engineering, Anhui University of Science and Technology, Huainan, Anhui, 232001, China,* [2]*Institute of Environment-Friendly Materials and Occupational Health of Anhui University of Science and Technology (Wuhu), Wuhu, 241003, China and* [3]*State Key Laboratory of Mining Response and Disaster Prevention and Control in Deep Coal Mines, Anhui University of Science and Technology, Huainan 232001, China*

(Received 2 July 2020, revised 6 February, accepted 8 February 2021)

Abstract: In this study, a simple fluorescent chemosensor with good fluorescence properties was synthesized, and was used to develop a sensitive and selective sensor, for the determination of 2,4,6-trinitrophenol (TNP) and Ag^+ in THF/H_2O medium, based on the fluorescence quenching mechanism. Fluorescence quenching experiments revealed that the fluorescence intensities of the resulted probe were linear with the concentrations of TNP and Ag^+ in the concentration range of 3.0–5.0 and 2.0–5.0 μmol dm^{-3}, with the detection limit of 1.36 and 0.82 μmol dm^{-3}, respectively. At the same time, accompanied with fluorescent color change under 365 nm UV light irradiation. This has demonstrated that the compound can act as a potential candidate for a "naked-eye" rapidly detector for Ag^+ and TNP in soils and aquatic systems.

Keywords: benzimidazole; quinoline; fluorescence quenching; TNP.

INTRODUCTION

2,4,6-Trinitrophenol (TNP), a nitroaromatic explosives (NAEs) are more violent and explosive than its another analogue. It features better solubility, stronger toxicity and explosive power even at very low concentrations, that may contaminate groundwater and cause many serious diseases.[1,2] On the other hand, silver ion, like other heavy metal ions, is widely used in industry and agriculture hence a large amount of Ag^+ has been introduced into surface water. Because it can inactivate cellular enzymes by binding with amino, and thiol groups or by triggering oxidative damage, Ag^+ has been recognized as one of the most hazardous heavy metal pollutants,[3] with great influence on people's health and bio-

* Corresponding author. E-mail: wb6314005@126.com; 2834846807@qq.com
https://doi.org/10.2298/JSC200702009W

logical systems.[4] Hence, accurate determination of trace Ag^+ and TNP in environmental samples is important for environmental monitoring. Toward this purpose, different techniques have been developed to determine NAEs including mass spectrometry,[5,6] gas chromatography (GC),[7] ion mobility spectrometry (IMS) and thermal neutron analysis, *etc*.[8,9] Many conventional methods, such as flame atomic absorption, potentiometry, voltammetry and inductively coupled plasma atomic emission spectrometry, are widely used to detect Ag^+ too. Unfortunately, some detecting techniques are expensive and cannot satisfy the demand of real-time detection.[10] The fluorescent detection has become popular because of its operational simplicity, high selectivity, good sensitivity, rapidity, nondestructive methodology, direct visual perception, *etc.*[11] In view of the above, design and synthesis of new fluorescent chemosensors for the efficient detection of TNP and Ag^+ is one of the most important research topics in environmental chemistry and biology.

Quinoline and imidazole have attracted tremendous attention because the nitrogen atom can act as a chelating site towards metal ions. The aromatic heterocyclic quinoline, as one of the most widely used organic optoelectronic functional materials, it undergoes π–π* electronic transition, and exhibits strong fluorescence.[12] Owing to the benzene ring and the imidazole ring being heterocyclic coplanar, benzimidazole presents unique electronic distribution and forms a big π-bond system, which is a well-known chromophore used in fluorescence sensing.[13] Compared with the other nitro compounds, TNP not only has a strong electron-withdrawing ability, but also has a strong light absorption capacity at a large excitation wavelength. Based on this consideration, the benzimidazole and quinoline were combined into a molecule (BAQ) to increase the selectivity and sensitivity for detection metal ions and TNP. Furthermore, the probe showed high sensitivity and selectivity for TNP and Ag^+ in THF/H_2O mixed solution. The extraordinary sensing properties endowed the compound with sensitive fluorometric chemosensors for the potential application of TNP and Ag^+ detection in environment system.

EXPERIMENTAL

Materials

All chemicals used in this work were analytical reagent grade, purchased from Aladdin Reagent Co. Ltd. (Shanghai, China), and used without further treatment. Deionized water (18 MΩ cm) from a water purification system was used in this experiment.

Synthesis of fluorescent probe

The synthesis route of BAQ (2,2′-di(quinolin-2-yl)-1*H*,1′*H*-5,5′-bibenzo[*d*]imidazole) is shown in Scheme 1.[14]

Briefly, 0.0132 mol of quinoline-2-carboxylic acid and 0.006 mol of biphenyl-3,4,3',4'--tetraamine were dissolved in polyphosphate (25 mL), The mixture was refluxed for 48 h at 160 °C, the reaction was stopped by adding distilled water, and then cooled to room tem-

perature. Then, the pH value of the solution was adjusted to 9–10 with sodium hydroxide. The brown powder was collected by vacuum filtration, further purification was accomplished by recrystallization from anhydrous ethanol, melting point 183–185 °C (yield: 83.6 %).

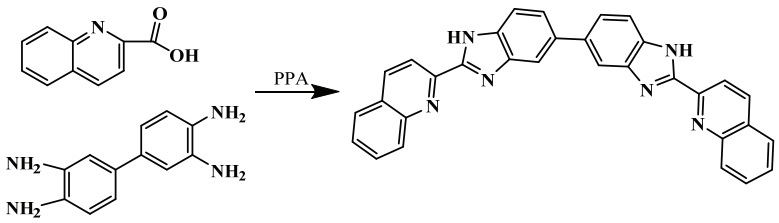

Scheme 1. Synthetic route for probe BAQ.

Characterization

Fourier transform infrared spectroscopy (FT-IR) measurements were performed on a Bruker Vector-22 FT-IR spectrometer. Each vacuum-dried sample was ground with KBr and compressed into a pellet.

^{1}H-NMR spectral data were recorded on Agilent Technologies 400 spectrometer (400 MHz) with DMSO-d_6 as solvent and TMS as internal standard.

The fluorescence experiments were performed at room temperature with the major equipment Perkin-Elmer F-4600 spectrofluorometer.

RESULTS AND DISCUSSION

FT-IR and NMR analyses

The probe was characterized by ^{1}H-NMR and FT-IR spectra. In Fig. 1a, ^{1}H--NMR (400 MHz, DMSO-d_6, δ / ppm) typical peaks are observed at 7.61–7.79 (*m*, 6H), 7.95–7.85 (*m*, 4H), 8.07–8.12 (*d*, J = 8.1 Hz, 2H), 8.17–8.25 (*d*, J = = 8.3 Hz, 2H), 8.50–8.63 (*m*, 4H), 13.30 (*s*, 2H). As shown in Fig. 1b, the FT-IR spectrum exhibits: –NH (3421 cm^{-1}), aromatic C–H (3060 cm^{-1}),[15] C=N stretching vibration (1590 cm^{-1}), C–N (1301 and 833 cm^{-1}),[16,17] the ring vibrations of benzimidazole and quinolin (1502, 1438, 1409, 1106 and 757 cm^{-1}).[18]

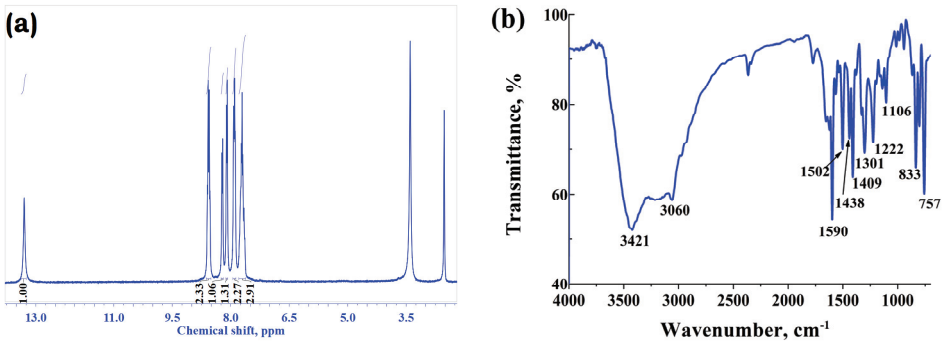

Fig. 1. ^{1}H-NMR (a) and FT-IR (b) spectra of the BAQ.

Fluorescence detection of TNP

Based on the better photoluminescence properties and the larger excitation wavelengths for BAQ, we investigated its sensing properties towards the potential explosive TNP. A stock solution of BAQ was prepared in THF/H_2O (1:1 volume ratio). The solutions of various NACs including trinitrotoluene (TNT), 4-nitrotoluene (4-NT), 2,6-dinitrotoluene (2,6-DNT), 2,4-dinitrotoluene (2,4-DNT), 4-nitrophenol (4-NP), 2-nitrophenol (2-NP), nitrobenzene (NB), 2-nitrotoluene (2-NT) and 2,4,6-trinitrophenol (TNP) were prepared in mixed solvent (THF/ /H_2O, 1:1 volume ratio). Nitroaromatic explosive (10^{-3} mol dm^{-3}) was mixed separately with equal volume BAQ solution (10^{-4} mol dm^{-3}), the blank sample was prepared with BAQ solution and equal volume of mixed solvent. All spectra were measured for 10 min after addition of the NAE with excitation wavelength 369 nm at room temperature, and emission was collected from 389 to 650 nm. The slit widths of the excitation and emission were both 5 nm. Fig. 2a shows that TNP caused the obvious fluorescence quenching accompanied with fluorescent color changes from light blue to turquoise under 365 nm UV lamp. The solution color did not change upon the addition of other NAEs, the apparent fluorescence emission change could be distinguished by the naked eye. These results indicate that BAQ possesses high selectivity for TNP sensing.

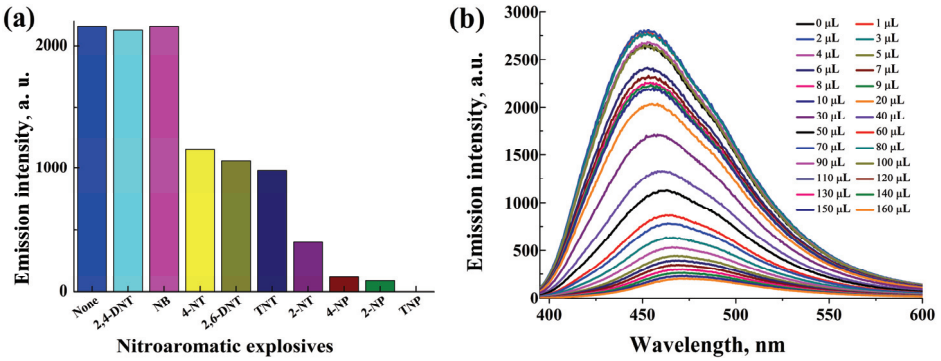

Fig. 2. Fluorescence spectra bar graph representation of the probe solution upon addition of various NAEs (a) and fluorescence spectra changes of the probe solution upon addition of different amounts of TNP (b).

To further evaluate the sensing properties of BAQ toward TNP, fluorescence quenching titration studies were carried out by progressive addition of TNP (THF/H_2O, 1:1 volume ratio). The solution of TNP (10^{-3} mol dm^{-3}) was gradually titrated into 2 mL stock solution of BAQ (2 mL, 10^{-4} mol dm^{-3}). As depicted in Fig. 2b, with the gradual addition of TNP, the fluorescence intensities gradually decreased. Based on the fluorescence titration results, the sensitivity of the probe to detect TNP is evaluated by the Stern–Volmer equation:

$$(I_0/I) - 1 = K_{SV}[Q] \quad (1)$$

where K_{SV} is Stern–Volmer constant indicating the sensitivity of probe; I_0 and I are the fluorescence intensities before and after the addition of TNP at 452 nm (total volume change negligible), [Q] is the molar concentration of TNP. According to Stern–Volmer, the ratio of fluorescence intensity in the absence and presence of TNP displays a linear response ($R^2 = 0.988$) to the TNP concentration in the range of 3.0–5.0 μmol dm^{-3} (Fig. 3a), and the corresponding constant K_{SV} for the TNP probe was calculated as 7.07×10^4 dm^3 mol^{-1}. The limit of detection (*LOD*) was calculated to be 1.36 μmol dm^{-3}, which was determined with the following equation:

$$LOD = \frac{3\delta}{D} \quad (2)$$

The δ was the standard deviation of blank measurements; D was the slope between fluorescence intensity and TNP concentration.[19] The comparison between our probe and the reports has been added in the Table I, which confirmed the high sensitivities of the chemsensors.[20–23] These results demonstrate that BAQ can be applied as a kind of probe for TNP sensing.

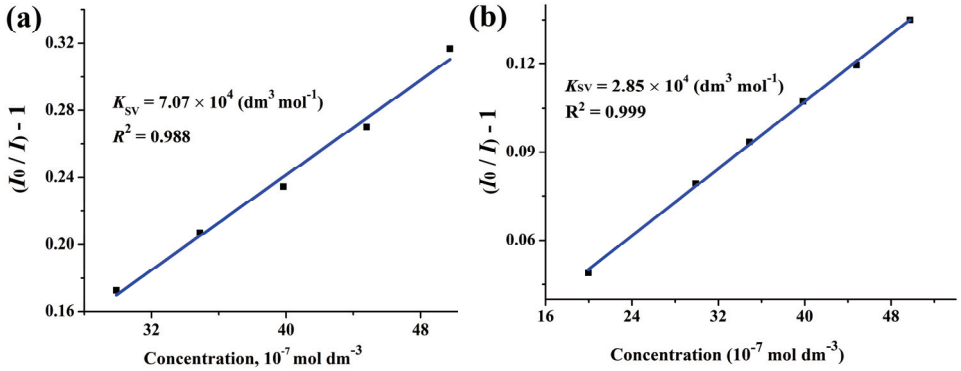

Fig. 3. The Stern–Volmer plot of BAQ for quenching of TNP (a) and Ag^+ (b).

Fluorescence detection of Ag^+

The optical properties of BAQ induced by metal ions also were studied in mixed solvent (THF/H_2O, 1:1 volume ratio) at room temperature. The solutions of metal ions (Mg^{2+}, K^+, Ca^{2+}, Al^{3+}, Cr^{3+}, Fe^{3+}, Co^{2+}, Cu^{2+}, Zn^{2+} and Ag^+) were prepared by the dissolution of their corresponding nitrate salts in THF/H_2O. Each metal ion solution (10^{-3} mol dm^{-3}) was mixed with equal volume of BAQ solution (10^{-4} mol dm^{-3}), the blank sample was prepared with BAQ solution and equal volume of mixed solvent. All spectra were measured for 10 min after addition of the metal ion solution with excitation wavelength 369 nm at room tempe-

TABLE I. Comparison of different chemosensors for the detection of TNP

Chemosensor	Formula	*LOD* / μmol dm^{-3}	Reference
Gelators with pyridine	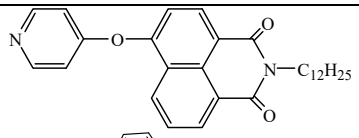	0.64	20
Nph-An derivative	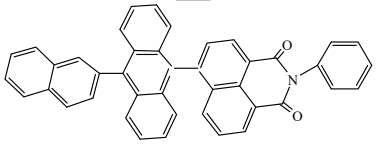	470	21
Quinine sulphate	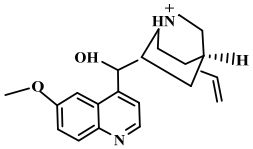	1.98	22
Carbon quantum dots		1.8	23
Benzimidazole derivatives		1.36	This work

rature, and emission was collected from 389 to 650 nm. The slit widths of the excitation and emission were both 5 nm. Fig. 4a showed the fluorescence spectra changes stimulated by Mg^{2+}, K^{+}, Ca^{2+}, Al^{3+}, Cr^{3+}, Fe^{3+}, Co^{2+}, Cu^{2+}, Zn^{2+} and Ag^{+}, these metal ions exhibit different degree of quenching on the fluorescence intensities. However, Ag^{+} not only caused the obvious fluorescence quenching, but also were accompanied with fluorescent color change from light blue to turquoise under 365 nm UV light irradiation. Therefore, BAQ has excellent selectivity for the detection of Ag^{+}.

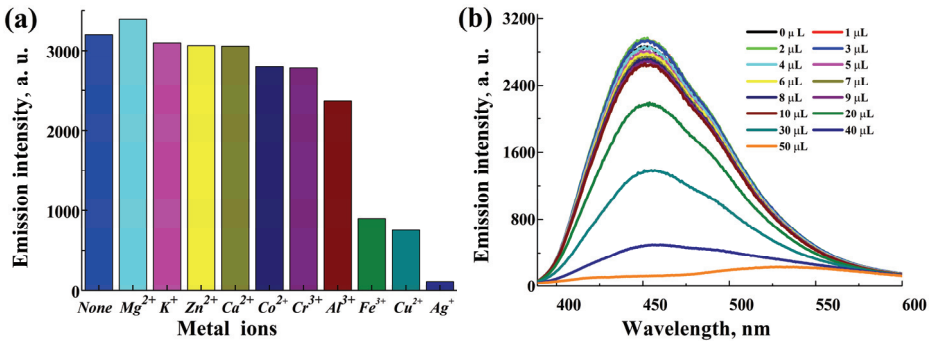

Fig. 4. Fluorescence spectra bar graph representation of the probe solution upon addition of various metal cations (a) and fluorescence spectra changes of the probe solution upon addition of different amounts of Ag^{+} (b).

To further evaluate the sensing properties of BAQ toward Ag^{+}, the emission spectra of BAQ titration experiments for Ag^{+} were carried out. The solution of

Ag^+ (10^{-3} mol dm^{-3}) was gradually titrated into 2 mL stock solution of BAQ (10^{-4} mol dm^{-3}). As shown in Fig. 4b, the emission intensities gradually decreased with the increasing concentrations of Ag^+, which could be assigned to a combination effect enhanced fluorescence between Ag^+ and BAQ.[24] The significant changes in fluorescence were observed from light blue to turquoise under 365 nm UV lamp. The sensitivity of the probe to detect Ag^+ is evaluated by the Stern–Volmer equation too, the ratio of fluorescence intensity at 451 nm in the absence and presence of Ag^+ displays a linear response to the Ag^+ concentration in the range of (2.0–5.0 μmol dm^{-3} (R^2 = 0.999), with the K_{SV} value of 2.85×10^4 dm^3 mol^{-1} (as shown in Fig. 3b). The detection limit of BAQ for Ag^+ was 0.82 μmol dm^{-3}. According to the standards of the U.S. Environmental Protection Agency (EPA), the maximum content of Ag^+ in drinking water must be limited to 0.93 μmol dm^{-3}. Furthermore, the low detection limit of the chemosensor BAQ made it possible to detect the level of Ag^+ in drinking water in normal individuals as defined.[25] The comparison between our probe and the reports have been added in the Table II,[26–29] which indicated that the detection limit of BAQ is comparable or better than some similar fluorescent probes literature reported.

Job's plots experiments were carried out to elucidate the binding modes of BAQ with Ag^+. The analysis based on keeping the total concentration of BAQ and Ag^+ at 10^{-4} mol dm^{-3} and changing the molar fraction of Ag^+ (c_{Ag^+}) from 0 to 1.0.

TABLE II. Comparison of different chemosensors for the detection of silver ion

Chemosensor	Formula	*LOD* / μM	Reference
Conjugated polymers	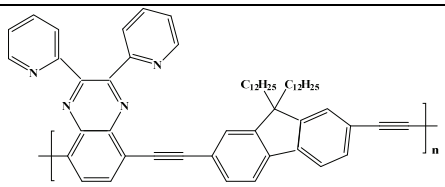	0.5	26
Gold nanoparticles (AuNPs)		1.0	27
NBD	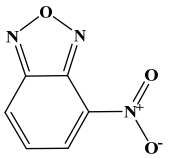	0.65	28
TPE-4DDC	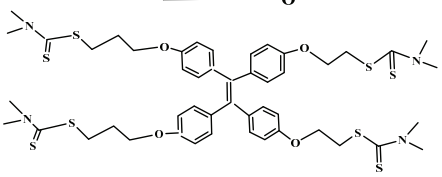	0.87	29
Benzimidazole derivative		0.82	This work

The difference in fluorescence intensity at 451 nm before (F_0) and after (F) the addition of Ag^+ was given as (F_0–F), As shown in Fig. 5a, the result shows that the F_0–F reached maximum at 451 nm at x_{Ag^+} of 0.5, indicating the formation of 1:1 complex of BAQ and Ag^+ based on the results of Job plot and the literature,[30] the plausible structure of Ag^++BAQ was shown in Fig. 5b, the benzimidazole and quinoline can cooperatively participate in the binding with Ag^+.[31]

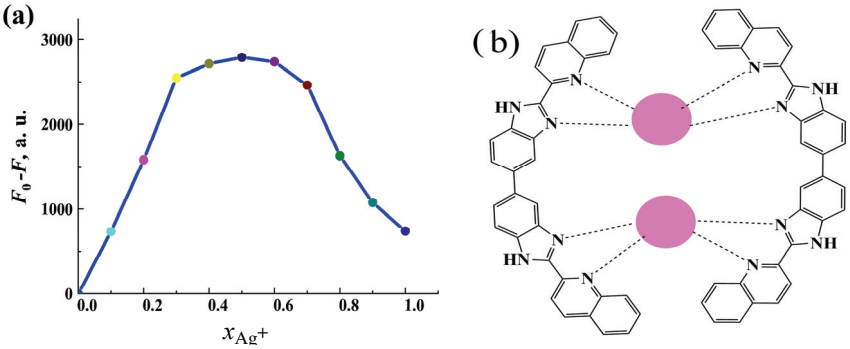

Fig. 5. Job plot of BAQ with Ag^+ complexation (a) and plausible structure of Ag^++BAQ (b).

Sensing mechanism of BAQ with Ag^+ and TNP

The common mechanism of the fluorescence detection is the photo-induced electron transfer (PET) and Förster resonance energy transfer (FRET).[32] PET includes electron move from LUMO of energized fluorophore to LUMO of quencher.[33] A productive PET can happen when the LUMO of fluorophore lie somewhat above in energy than LUMO of acceptor. We performed the theoretical research by employing the density functional theory (DFT) in Gaussian B3LYP/ /6-31g* basis set. The calculated HOMO–LUMO energy levels of the common NAEs and BAQ are summarized in Fig. 6a. NAEs are all electron deficient substances, the lower LUMO energy of BAQ signifies the stronger electron withdrawing ability and the higher quenching efficiency.

TNP shows the highest quenching efficiency because of the lowest LUMO among the NAEs. The result suggests that electron transfer can more easily occur from BAQ to TNP. Apart from this, the FRET could be identified by the overlap of the absorbance spectra of NAEs and the photoluminescence (PL) spectra of BAQ [34]. The absorption spectrum of TNP has large overlap with the PL spectrum of BAQ (Fig. 6b), which contributed to FRET from BAQ to TNP. Both the EET and FRET synergistically induce the fluorescence quenching of BAQ, resulting in the contribution of good sensing performance toward TNP, which could be the result of the formation of hydrogen binding between TNP guest and the nitrogen atoms on sensor. These could be attributed to the mechanism of electron and

resonance energy transfer processes in the complexes with the molecular interactions.[35,36]

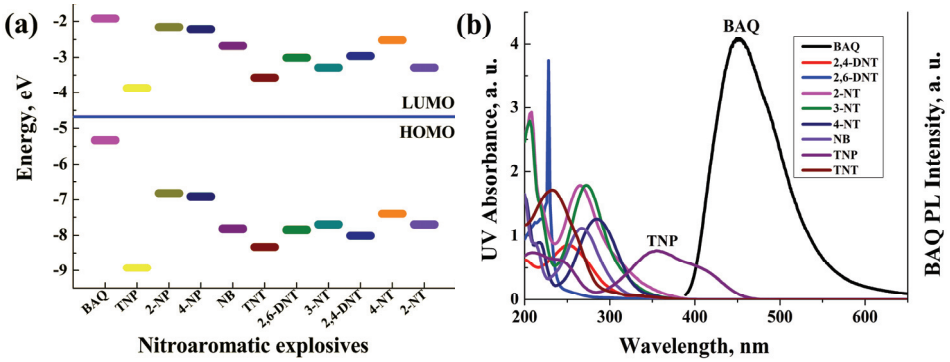

Fig. 6. Positions of the HOMO and LUMO energy levels of BAQ and various NAEs (a); spectral overlap between the PL spectrum of sensor BAQ and the absorption spectra of TNP (b).

UV-Vis absorption spectrum of BAQ (Fig. 7a) shows the typical absorption band at 216 nm (π-π transition) and 281 nm(π-π* transition).[37]

The UV–Vis absorbance spectrum of BAQ displayed significant change after addition of Ag^+, the absorbance band at 281 nm decreased largely accompanied by emerging of a new absorbance band in the range of 356~407 nm with a peak at 389 nm, which proved that BAQ formed a firmed binding with Ag^+. The significant changes in the UV–Vis spectra of macrocyclic compounds and their complexes with Ag^+ suggested the formation of ground-state complexes with charge transfer process. As appeared in Fig. 7b, the absorption spectrum of Ag^+ has no overlap with excitation spectra of BAQ. So these excellent performances of BAQ for Ag^+ and TNP detection could be mainly due to different mechanisms. For Ag^+ detection, the main mechanism is based on PET. While for TNP detection, the mechanism could be FRET and PET

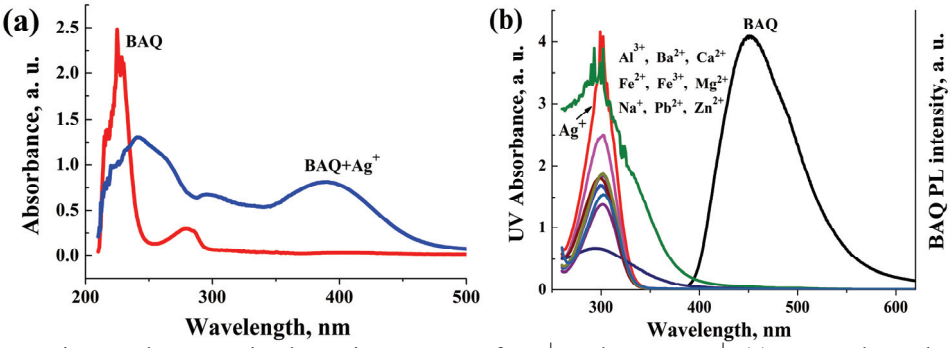

Fig. 7. The UV–Vis absorption spectra of Ag^+ and BAQ+Ag^+ (a); spectral overlap between the PL spectrum of sensor BAQ and the absorption spectra of Ag^+ (b).

CONCLUSIONS

In summary, we report the synthesis, structural characterization, photoluminescence behavior and the sensing properties of a novel chemosensor containing benzimidazole and quinolone units (BAQ). The sensing properties of BAQ toward the potential explosive TNP and Ag^+ were investigated. The detection selectivity of the compound for TNP and Ag^+ could be visualized by naked eyes in THF/H_2O solution, and the detection limits of TNP and Ag^+ were as low as 1.36 and 0.82 μmol dm^{-3}, respectively. At last, the detection mechanism of BAQ for Ag^+ and TNP detection were further investigated by the theoretical calculation, ultraviolet and fluorescence spectra. Based on the different detection mechanism, the BAQ exhibited different fluorescent response to Ag^+ and TNP. The results will help to design effective fluorometric sensors with benzimidazole and quinoline units in future.

Acknowledgements. This work was supported by the Funded by Research Foundation of the Institute of Environment-Friendly Materials and Occupational Health of Anhui University of Science and Technology (Wuhu) (Grant No. ALW2020YF06); the Key Research and Development Projects in Anhui Province (Grant No. 202004h07020022).

ИЗВОД

ФУНКЦИОНАЛНА ФЛУОРЕСЦЕНТНА ПРОБА НА БАЗИ БЕНЗИМИДАЗОЛА ЗА БРЗО ОДРЕЂИВАЊЕ 2,4,6-ТРИНИТРОФЕНОЛА И Ag^+ У СМЕШИ ТЕТРАХИДРОФУРАН–ВОДА

BIN WANG[1,2], FAN JIANG[1], XIXI ZUO[1], JING MA[1] И XIANGMEI MA[1,2]

[1]*Institute of Chemical Engineering, Anhui University of Science and Technology, Huainan, Anhui, 232001, China u* [2]*Institute of Environment-Friendly Materials and Occupational Health of Anhui University of Science and Technology (Wuhu), Wuhu, 241003, China*

У овом раду је описан новосинтетисан, једноставан и осетљив хемисензор, са добрим флуоресцентним карактеристикама, које су искоришћене за селективно одређивање 2,4,6-тринитрофенола (TNP) и Ag^+ у смеши THF/H_2O. Интензитет флуоресценције новосинтетисаног једињења линеарно опада у опсегу концентрација TNP 3,0––5,0 μmol dm^{-3} и Ag^+ 2,0–5,0 μmol dm^{-3}, са границом детекције од 1,36 μmol dm^{-3} за TNP и 0,82 μmol dm^{-3} за Ag^+. Како под утицајем UV зрачења таласне дужине 365 nm долази до промене флуоресцентне боје, ово једињење је потенцијални кандидат за брзу детекцију Ag^+ и TNP у земљишту и воденим системима.

(Примљено 2. јула 2020, ревидирано 6. фебруара, прихваћено 8. фебруара 2021)

REFERENCES

1. M. Rong, L. Lin, X. Song, T. Zhao, Y. Zhong, J. Yan, Y. Wang, X. Chen, *Anal. Chem.* **87** (2015) 1288 (http://refhub.elsevier.com/S0039-9140(19)30151-1/sbref5)
2. Y. Salinas, R. M. Máñez, M. D. Marcos, F. Sancenón, A. M. Costero, M. Parra, S. Gil, *Chem. Soc. Rev.* **41** (2012) 1261 (http://refhub.elsevier.com/S1386-1425(19)30973-4/sref1)

3. N. Pandeya, M. S. Mehatab, N. Fatmaa, S. Pant. *Luminescence* **205** (2019) 475 (https://doi.org/10.1016/j.jlumin.2018.09.062)
4. H. Y. Wang, Q. J. Lu, M. X, Li, H. Li, Y. L. Liu, H. T. Li, Y. Y. Zhang, S. H. Yao, *Anal. Chim. Acta* **1027** (2018) 121 (https://doi.org/10.1016/j.aca.2018.03.063)
5. L. Barron, E. Gilchrist, *Anal. Chim. Acta* **806** (2014) 27 (http://refhub.elsevier.com/S0039-9140(19)30151-1/sbref7)
6. K. Badjagbo, S. Sauve, *Anal. Chem.* **84** (2012) 5731 (http://refhub.elsevier.com/S0039-9140(19)30151-1/sbref8)
7. M. Berg, J. Bolotin, T. B. Hofstetter, *Anal. Chem.* **79** (2007) 2386 (http://refhub.elsevier.com/S0039-9140(19)30151-1/sbref9)
8. M. Sabo, S. Matejcik, *Anal. Chem.* **84** (2012) 5327 (http://refhub.elsevier.com/S0039-9140(19)30151-1/sbref14)
9. G. Vourvopoulos, P. Womble, *Talanta* **54** (2001) 459 (http://refhub.elsevier.com/S0039-9140(19)30151-1/sbref15)
10. J. H. Pang, K. Z. Shen, D. F. Ren, S. N. Feng, Y. Wang, Z. H. Jiang, *J. Mater. Chem.* **1** (2013) 1465 (https://doi.org/10.1039/C2TA00363E)
11. Y. Fu, P. Li, J. X. Kang, X. Y. Liu, G. Y. Li, F. Ye, *Luminescence* **178** (2016) 156 (http://dx.doi.org/10.1016/j.jlumin.2016.05.023)
12. L Liu, F Dan, W. Liu, X. Lu, Y. Han, S. Xiao, H. Lan. *Sensors Actuators, B* **247** (2017) 445 (http://dx.doi.org/10.1016/j.snb.2017.03.069)
13. R. M. Gadirov, R. R. Valiev, L. G. Samsonova, *Chem Phys Lett.* **717** (2019) 53 (https://doi.org/10.1016/j.cplett.2019.01.014)
14. X. C. Han, Y. J. Xie, D. Liu, *J Membrane Sci*. **589** (2019) 117230 (https://doi.org/10.1016/j.memsci.2019.117230)
15. S. Khatua, S. H. Choi, J. Lee, K. Kim, Y. Do, D. G. Churchill, *Inorg. Chem.* **48** (2009) 2993 (http://refhub.elsevier.com/S1386-1425(16)30586-8/rf0220)
16. 16. S. Khatua, J. Kang, D. G. Churchill, *New J. Chem.* 34 (2010) 1163 (http://refhub.elsevier.com/S1386-1425(16)30586-8/rf0230)
17. K. Wang, L. Ma, G. Liu, D. Cao, R. Guan, Z. Liu, *Dyes Pigments***126** (2016) 104 (http://10.1016/j.dyepig.2015.11.019)
18. K. Wang, W. Feng, Y. Wang, D. Cao, R. Guan, X. Yu, Q. Wu, *Inorg. Chem. Commun.* **71** (2016) 102 (http://dx.doi.org/10.1016/j.inoche.2016.07.013)
19. L. Wang, D. Ye, D. Cao, *Spectrochim. Acta A* **90** (2012) 40 (http://dx.doi.org/10.1016/j.saa.2012.01.017)
20. X. Cao, N. Zhao, H. Lv, Q. Ding, A. Gao, Q. Jing, T. Yi, *Langmuir* **33** (2017) 7788 (http://refhub.elsevier.com/S0039-9140(19)30151-1/sbref55)
21. H. Ma, C. He, X. Li, O. Ablikim, S. Zhang, M. Zhang, H. Ma, C. He, X. Li, O. Ablikim, S. Zhang, M. Zhang, *Sensors Actuators, B* **230** (2016) 746 (http://refhub.elsevier.com/S1386-1425(17)30131-2/rf0205)
22. J. Y. Du, J. P. Liu, Y. F. Ren, C. W. Wang, F. B. Bai, H. X. Hao. *Spectrochim. Acta, A* **211** (2019) 287 (https://doi.org/10.1016/j.saa.2018.12.014)
23. F. Cheng, X. An, C. Zheng, S. Cao, *RSC Adv*. **113** (2015) 93360 (https://doi.org/10.1039/C5RA19029K)
24. G. J. Park, H. Kim, J. J. Lee, Y. S. Kim, S. Y. Lee, S. Lee, I. Noh, C. Kim, *Sensorors Actuators, B* **215** (2015) 568 (http://refhub.elsevier.com/S0040-4020(16)30405-7/sref33)

25. Y. Tian, Y. Chen, M. Chen, Z. L. Song, B. Xiong, X. B. Zhang. *Talanta* **221** (2021) 121627 (https://doi.org/10.1016/j.talanta.2020.121627)
26. W. Cui, L. Y. Wang, G. Xiang, L, X. Zhou, X. N. An, D. R. Cao, *Sensorirs Actuators, B,* **207** (2015) 281 (http://dx.doi.org/10.1016/j.snb.2014.10.072)
27. B. Liu, H. Tan, Y. Chen, *Microchimica Acta* **180** (2013) 331 (http://refhub.elsevier.com/S0925-4005(18)30732-9/sbref0240)
28. Y. Fu, L. Mu, X. Zeng, J. L. Zhao, C. Redshaw, X. L. Ni, T. Yamatoc, *Dalton Trans.* **42** (2013) 3552 (http://refhub.elsevier.com/S2214-1804(15)30025-8/rf0160)
29. Y. Li, H. Yu, G. Shao, F. Gan. *J. Photochem. Photobiol., A* **301** (2015) 14 (http://dx.doi.org/10.1016/j.jphotochem.2014.12.013)
30. C. Chen, H. Liu, B, Zhang, Y, Wang, K, Cai,Y, Tan, C. Gao, H. Liu, C. Tan, Y. Jiang, *Tetrahedron* **72** (2016) 3980 (http://dx.doi.org/10.1016/j.tet.2016.05.020)
31. L. L. Liu, F. J. Dan, W. J. Liu, X. Lu, Y. L. Han, S. Z. Xiao, H. C. Lan, *Sensorors Actuators, B* **247** (2017) 445 (http://dx.doi.org/10.1016/j.snb.2017.03.069)
32. X. Hu, H. Zeng, T. Chen, H. Q. Yuan, L. Zeng, G.-M. Bao, *Sensors Actuators, B* **319** (2020) 1282829 (http://dx.doi.org/10.1016/j.snb.2020.128282)
33. S. Zhang, H. Wang, Y. Li, F. Y. Data, Q. Wang, L. Jiao, *Mater. Lett.* **263** (2020) 127208 (https://doi.org/10.1016/j.matlet.2019.127208)
34. H. Ma, F. Li, L. Yao, Y. Feng, Z. Zhang, M. Zhang, *Sensorors Actuators, B* **259** (2018) 380 (https://doi.org/10.1016/j.snb.2017.12.029)
35. S. Zhang, H. Wang, Y. Li, F. Y. Data, Q. Wang, L. Jiao, *Mater. Lett* **263** (2020) 127208 (https://doi.org/10.1016/j.matlet.2019.127208)
36. F. Qiu, Y. H. Huang, Q. M. Ge, M. Liu, H. Cong, Z. Tao. *Spectrochimica Acta, A* **226** (2020) 117583. (https://doi.org/10.1016/j.saa.2019.117583)
37. S. Philip, P. S. Thomas, K. Mohanan. *J. Serb. Chem. Soc.* **83** (2018) 561 (https://doi.org/10.2298/JSC180918010P).